Unique Directional Properties of Dual-Diaphragm Microphones

Guy Torio, Jeff Segota
Department of Acoustical Development
Shure Incorporated
Evanston, Illinois 60202, USA

Abstract - Dual-diaphragm condenser capsules are commonly used in popular multi-pattern microphones, as well as some single pattern unidirectional designs. These capsules react much differently to sound sources than single-diaphragm capsules in the frequency range up to approximately 1 kHz. As a method of developing intuition, frequency response and directionality as a function of distance from the sound source are demonstrated using a simple model. Pop sensitivity and multi-pattern operation are also investigated. Comparisons and conclusions are validated with measurements made on physical microphones.

1. INTRODUCTION

A practical and effective method for implementing multiple directional responses in a condenser microphone is to use a dual-diaphragm capsule. Since its invention by Von Braummuhl and Weber in the 1930's [1], numerous manufacturers have used this approach to produce many popular and commonly used studio microphones. Also, several single pattern designs contain dual-diaphragm capsules.

The frequency and polar responses of directional microphones are dependent upon proximity of the sound source, particularly at frequencies below 1 kHz. This subject has been studied for the case of a single-diaphragm condenser capsule [2]. Dual-diaphragm condenser capsules respond differently, however, and this can have real implications in certain applications. The main purpose of this study is to derive and measure the effect of source proximity on the frequency and polar responses of a dual-diaphragm condenser capsule operating as a cardioid, and to compare the results to that of a single-diaphragm cardioid capsule. The differences are analyzed in order to gain an understanding of how the two will perform differently in typical applications.

The lumped-element, equivalent circuit model for a single-diaphragm capsule is reviewed [2], and a model for the dual-diaphragm capsule is derived. From these, transfer functions are obtained for the point source case. Each function contains two terms, one that is dependent on source proximity and one that is not, and it is the source proximity dependent term that differentiates the single and dual-diaphragm capsules. Polar and frequency response plots for various source distances are generated from the transfer functions, and the results are confirmed with measured data. The responses are discussed in terms of how the single and dual-diaphragm capsules will perform differently in particular applications.

In addition, the results of pop sensitivity measurements for the single and dual-diaphragm cardioid capsules are presented and discussed. And lastly, the frequency response of the dual-diaphragm capsule in figure-of-eight and omnidirectional operation as a function of distance is analyzed.

2. THE SINGLE-DIAPHRAGM MODEL

The model for the single-diaphragm cardioid condenser capsule is developed in this section. A simple capsule is shown in cross-section in Fig. 1. The diaphragm vibrates as a result of a difference between the sound pressures on the front and back. The capsule output is proportional to the change in capacitance between the diaphragm and back plate resulting from diaphragm motion.

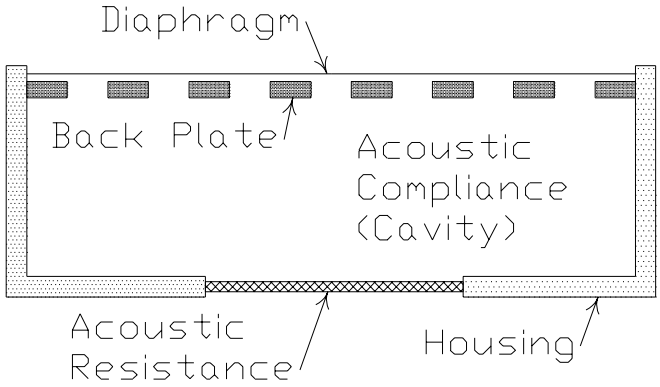

Fig. 1. Single-Diaphragm Cardioid Capsule.

A conceptual diagram showing how cardioid directionality is achieved is shown in Fig. 2. Sound reaching the back of the capsule passes through an acoustic circuit consisting of a resistance R_a and a compliance (cavity) C_a to the back of the diaphragm. This circuit is a low-pass filter, imparting a phase lag for frequencies below the knee of the filter. This phase lag is referred to as the internal phase shift, and the circuit is referred to as the acoustic phase shift network. Because sound travels at a finite speed, the sound pressure at the back of the capsule is time-shifted with respect to the sound pressure at the front of the capsule. This time shift, referred to as the external time delay, is a function of the sound wave incidence angle and the distance d between the front and back of the capsule. By choosing appropriate values for R_a and C_a, the internal phase shift is made to match the phase shift associated with the external time delay for the case of 180 degree sound incidence. Thus, a plane sound wave arriving from back of the capsule will reach both the front and back of the diaphragm in phase, resulting in zero net force and thus no diaphragm motion and no output. As the incidence angle varies so does the external time delay, resulting in a phase difference between the sound pressures at the front and back of the diaphragm. At zero degrees incidence this phase difference, and thus the force on the diaphragm and the capsule output, is maximum. Cardioid directionality is maintained as long as the incident sound wave is planar. The model will show how the directionality deviates for spherical sources in close proximity.

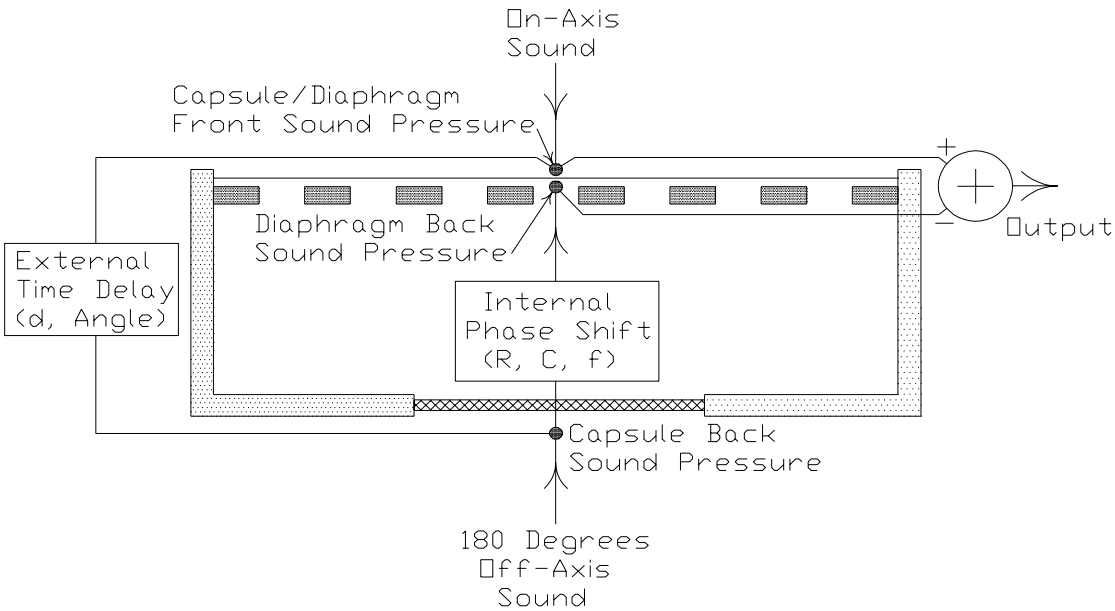

Fig. 2. Cardioid Operation Diagram.

The equivalent circuit of the acoustical/mechanical system in the low to mid frequency range is given in Fig. 3 [2].

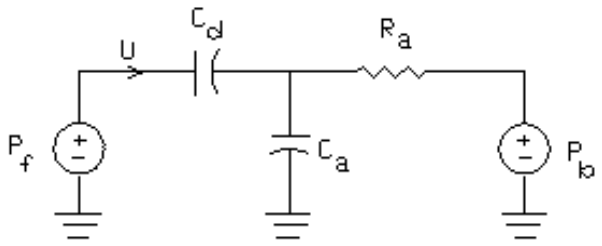

Fig. 3. Single-Diaphragm Capsule Equivalent Circuit.

As discussed in Section 3.2 of [2], the diaphragm is stiffness controlled in the frequency range of interest so it is modeled simply as an acoustic compliance C_d. C_a and R_a represent the compliance and resistance of the acoustic phase shift network. The sources represent the sound pressures at the front and back of the capsule. For a point source located at distance r and at angle θ with respect to the primary axis, the transfer function relating the capsule output to the front sound pressure is

$$\frac{e_o}{P_f} = K_{AE} \frac{sR_aC_a\left(1+\frac{d}{cR_aC_a}\cos(\theta)\right)+\frac{d}{r}\cos(\theta)}{sR_a(C_d+C_a)+1} \quad . \tag{1}$$

In the expression above, s represents complex frequency $j\omega$, and K_{AE} is a constant term representing the acoustical to electrical coupling.

From a systems perspective, (1) represents the sum of a first-order high-pass and low-pass filter that share the same cutoff frequency

$$f_{o\_SD} = \frac{1}{2\pi[R_a(C_a+C_d)]} \; . \tag{2}$$

Above the cutoff frequency, the high-pass filter gain is given by the expression

$$K_{HP\_SD} = \frac{C_a}{C_a+C_d}\left(1+\frac{d}{cR_aC_a}\cos(\theta)\right). \tag{3}$$

Below the cutoff frequency, the low-pass filter gain is given by the expression

$$K_{LP\_SD} = \frac{d}{r}\cos(\theta). \tag{4}$$

The complete system transfer function is illustrated in the block diagram in Fig. 4.

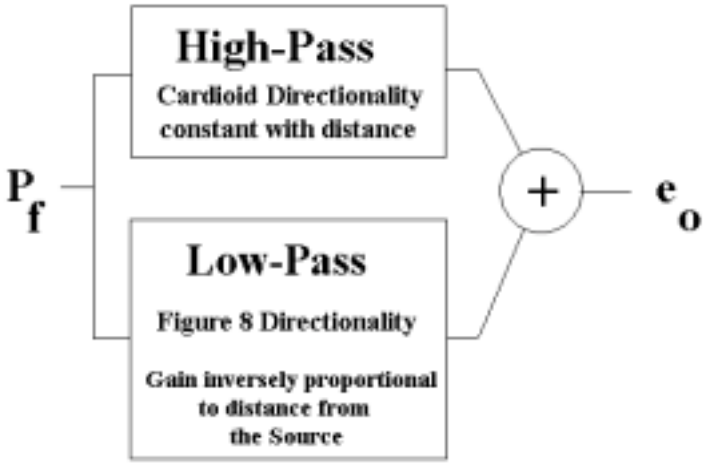

Fig. 4. Single-Diaphragm Capsule Transfer Function Block Diagram.

The high-pass portion is independent of source distance and has cardioid directionality. It also represents the far field, plane wave response. The low-pass portion represents the proximity effect term, having more gain the closer the capsule is to the point source. In addition, the polar response is bidirectional. Consequently, it will be shown that as source distance is reduced, the low frequency response is accentuated, and the polar response shifts from cardioid towards figure-of-eight.

3. THE DUAL-DIAPHRAGM MODEL

The model for the dual-diaphragm cardioid capsule is developed in this section. A simple capsule is shown in cross-section in Fig. 5. For cardioid operation, the output signal is taken across the front diaphragm and back plate. In addition to the elements contained in the single-diaphragm capsule, the acoustic phase shift network now contains the second diaphragm and the second compliance. It is the additional diaphragm that gives the capsule its unique properties at low frequencies. See Section 2 for an intuitive explanation of how the phase shift network is used to achieve cardioid directionality.

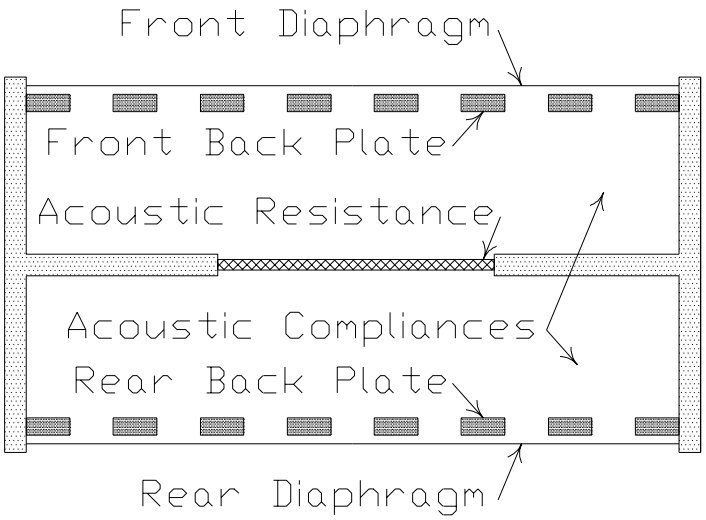

Fig. 5. Dual-Diaphragm Capsule.

The equivalent circuit of the acoustical/mechanical system in the low to mid frequency range is given in Fig. 6.

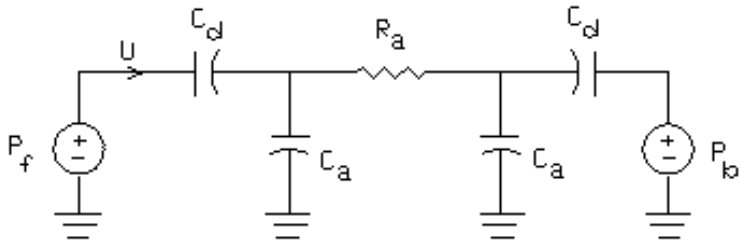

Fig. 6. Dual-Diaphragm Capsule Equivalent Circuit.

As discussed in Section 3.2 of [2], the diaphragms are stiffness controlled in the frequency range of interest so they are modeled simply as an acoustic compliance C_d. C_a and R_a represent the compliances and resistance of the acoustic phase shift network. The sources represent the sound pressures at the front and back of the capsule. For a point source located at distance r and at angle θ with respect to the primary axis, the transfer function relating the capsule output to the front sound pressure is (see Appendix for the derivation)

$$\frac{e_o}{P_f} = K_{AE}\frac{C_a C_d}{C_a + C_d}\frac{s\frac{R_a(C_a+C_d)}{2}\left(1+\frac{d}{cR_a\left(C_a+\frac{C_a^2}{C_d}\right)}\cos(\theta)\right)+\left(1+\frac{C_d}{2C_a}\frac{d}{r}\cos(\theta)\right)}{s\frac{R_a(C_d+C_a)}{2}+1}. \quad (5)$$

In the expression above, s represents complex frequency $j2\pi f$ (f = frequency in Hz), and K_{AE} is a constant term representing the acoustical to electrical coupling. From a systems perspective, (6) represents the sum of a first-order high-pass and low-pass filter that share the same cutoff frequency (two times higher than the single diaphragm case).

$$f_{o\_DD} = \frac{1}{\pi[R_a(C_a + C_d)]}. \quad (6)$$

Above the cutoff frequency, the high-pass filter gain is given by the expression

$$K_{HP\_DD} = \left(1+\frac{d}{cR_a\left(C_a+\frac{C_a^2}{C_d}\right)}\cos(\theta)\right). \quad (7)$$

Below the cutoff frequency, the low-pass filter gain is given by the expression

$$K_{LP\_DD} = \left(1 + \frac{d}{r}\frac{C_d}{2C_a}\cos(\theta)\right). \tag{8}$$

The complete system transfer function is illustrated in the block diagram in Fig. 7.

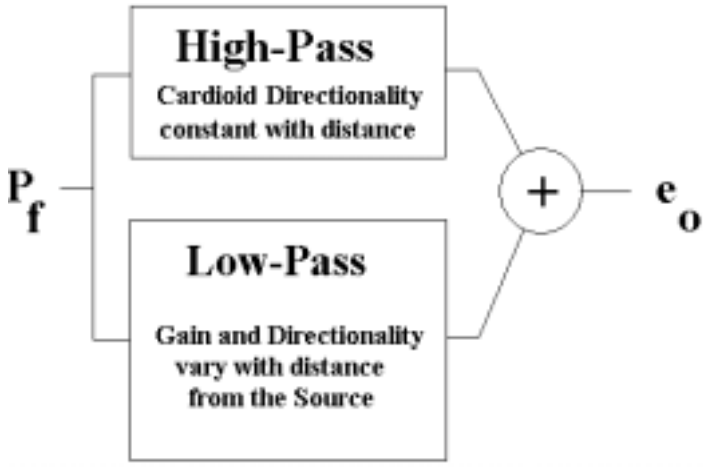

Fig. 7. Dual-Diaphragm Capsule Transfer Function Block Diagram.

As in the single-diaphragm case, the high-pass term has cardioid directionality and is independent of source distance. Also like the single-diaphragm capsule, the low-pass gain is source proximity dependent, but in this case its influence does not become diminished in the far field. Another difference is that the directionality of the low-pass term varies with source distance, tending toward omnidirectional in the far field and bidirectional in the near field. It is cardioid at an intermediate distance given by the expression

$$r = d\frac{C_d}{2C_a}\ . \tag{9}$$

4. MODEL COMPARISON

As a basis for comparison, polar and frequency responses are generated from the transfer functions derived in the previous two sections using the following parameter values:

d = 3.2 cm (1.25 inches)

C_d = 1.64 x 10^{-10} m^5/N

R_a = 200 x 10^5 MKS ohms

C_a = 5.3 x 10^{-12} m^5/N

Using these values, the high-pass portions of the transfer functions have cardioid directionality. Substituting into equations (2) and (6), the cutoff frequencies for the high-pass and low-pass terms for the single and dual-diaphragm models are 53 Hz and 106 Hz, respectively. Note that since the filter terms are first order, they will still have an influence on the opposite sides of their cutoff frequencies.

Fig. 8 shows the polar responses for an 8 feet source distance. This distance is fairly representative of far-field conditions, since the sound waves are essentially planar at all frequencies down to about 100 Hz. At 1 kHz, both models have very strong cardioid directionality. At 100 Hz, the single-diaphragm model still has a good cardiod pattern, because the influence of the low-pass portion of the transfer function is diminished at this distance. The dual-diaphragm model is leaning toward omnidirectional at 100 Hz, because the low-pass portion of the transfer function is strongly omnidirectional at this distance.

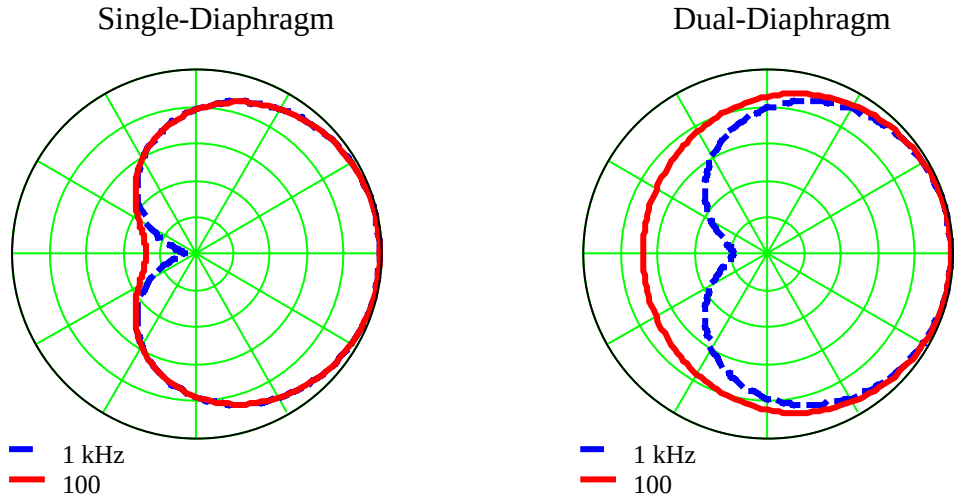

Fig. 8. Modeled Polar Responses, 8 Feet Source Distance (5 dB per division).

Fig. 9 shows the polar responses for a two feet source distance. At this distance sound waves are approximately planar at frequencies down to about 400 Hz. For the single-diaphragm model, the low-pass portion now has a stronger influence, and consequently the polar response at 100 Hz has shifted toward bidirectional. The dual-diaphragm model is a very strong cardioid at 100 Hz, because the low-pass portion of the transfer function is very close to cardioid at this distance (solving equation (9) for the parameter values above gives a distance of 1.62 feet).

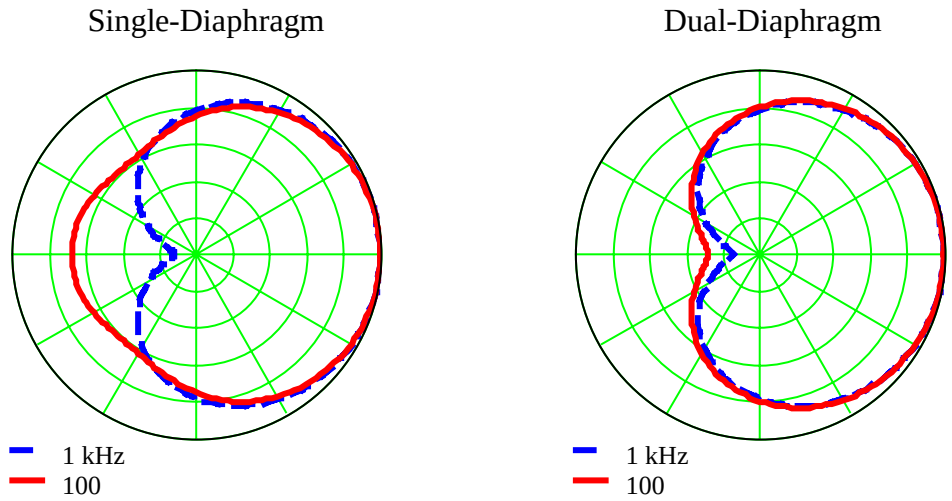

Fig. 9. Modeled Polar Responses, 2 Feet Source Distance (5 dB per division).

Fig. 10 shows the polar responses for a 6 inch source distance. This distance is representative of near-field conditions in the frequency range of interest, since the sound waves are essentially planar only at frequencies above about 1600 Hz. For the single-diaphragm model, the low-pass portion now has a very strong influence, as the polar response at 100 Hz is almost purely bidirectional and even at 1 kHz the pattern has shifted significantly away from cardioid. The dual-diaphragm model at 100 Hz has shifted beyond cardioid directionality to approximately supercardioid, due to the stronger influence and the change in directionality of the low-pass portion from cardioid towards bidirectional. Due to the close source proximity the low-pass term is also influencing the dual-diaphragm pattern at 1 kHz, shifting it slightly in the bidirectional direction (although this may be hard to see due to the limited resolution of the plot).

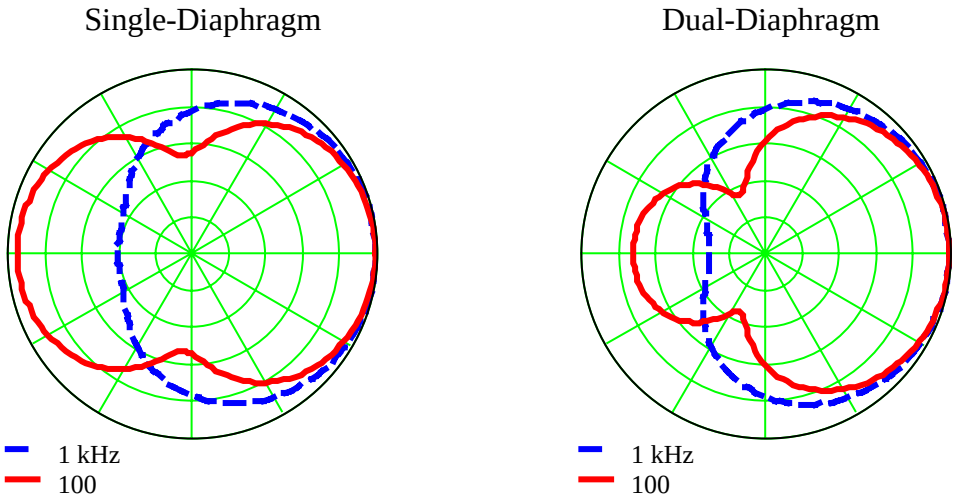

Fig. 10. Modeled Polar Responses, 6 Inch Source Distance (5 dB per division).

Another way to interpret the models is to look at their frequency responses as a function of sound incidence angle at different source distances, and these are shown in the following figures. The frequency range is 50 Hz to 3 kHz and the sound incidence angles are 0, 90, and 180 degrees. Fig. 11 shows single-diaphragm model response for an 8 feet source distance. The closeness in shape of the 0 and 90 degree sound incidence responses and the fairly low response for 180 degrees sound incidence (compared to closer source distances, to be seen) indicates a good cardioid pattern even at low frequencies. Thus, the effect of the low-pass, or source proximity term of the transfer function is minimal.

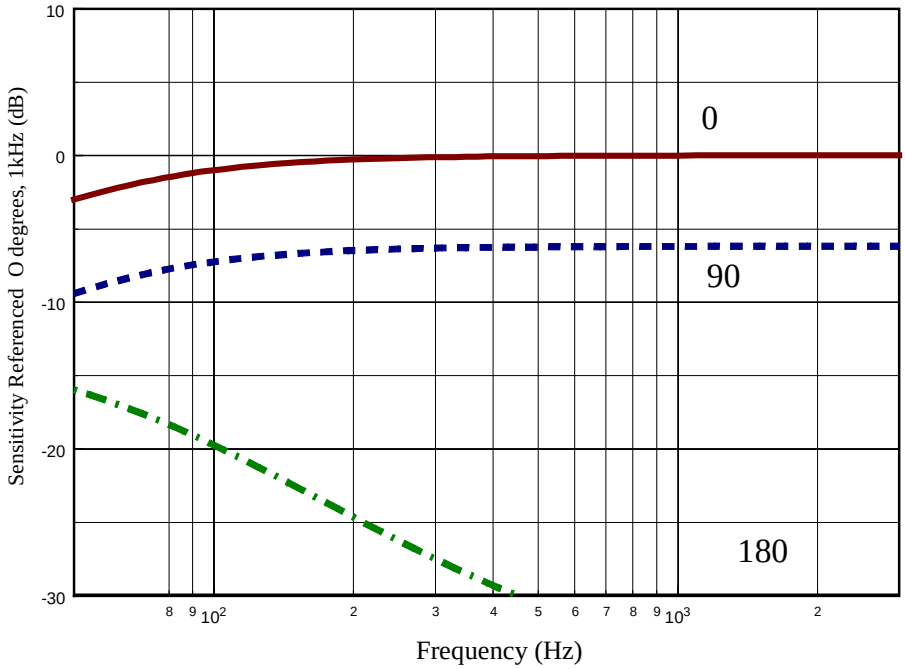

Fig. 11. Frequency Response, Single-Diaphragm Model, 8 Feet Source Distance.

Fig. 12 shows the dual-diaphragm model frequency response for an 8 feet source distance. The responses at the three incidence angles get closer to each other as the frequency is lowered, indicating a shift in directionality from cardioid towards omnidirectional. At this source distance, the low-pass, or source proximity term has a significant influence.

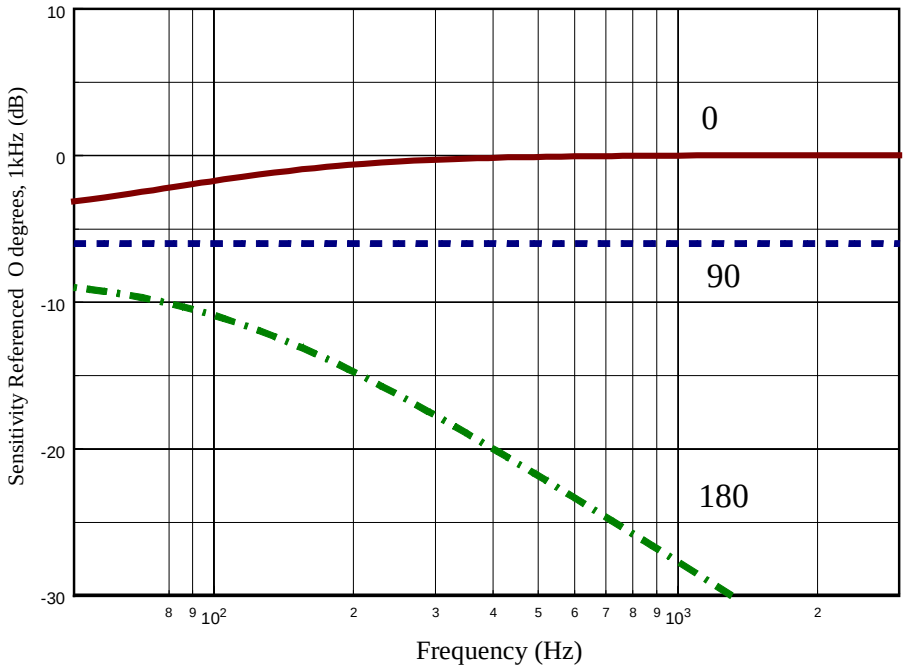

Fig. 12. Frequency Response, Dual-Diaphragm Model, 8 Feet Source Distance.

Fig. 13 shows the single-diaphragm model frequency response for a 2 feet source distance. Compared to the 8 feet source distance result, at low frequencies the 180 degree response is higher, and the 0 degree response is boosted. This indicates a shift in the directionality towards bidirectional. Thus, the low-pass term of the transfer function is starting to have an effect at this distance.

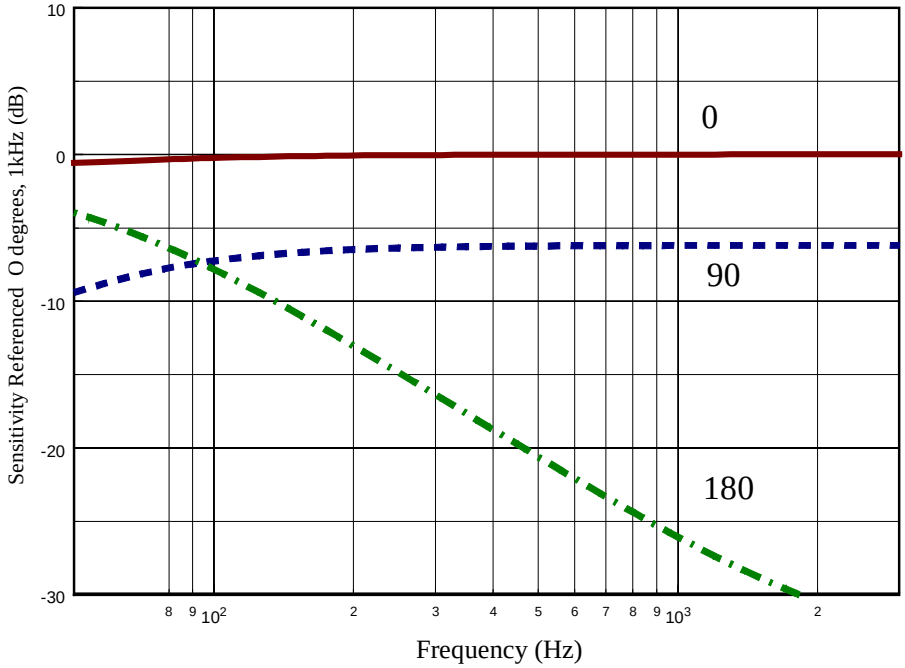

Fig. 13. Frequency Response, Single-Diaphragm Model, 2 Feet Source Distance.

Fig. 14 shows the dual-diaphragm model frequency response for a 2 feet source distance. The relatively close shape of the 0 and 90 degree sound incidence responses and the very low response for 180 degrees sound incidence indicates a strong cardioid pattern even at low frequencies. As discussed before, this is because the low-pass portion of the transfer function is very close to cardioid at this distance.

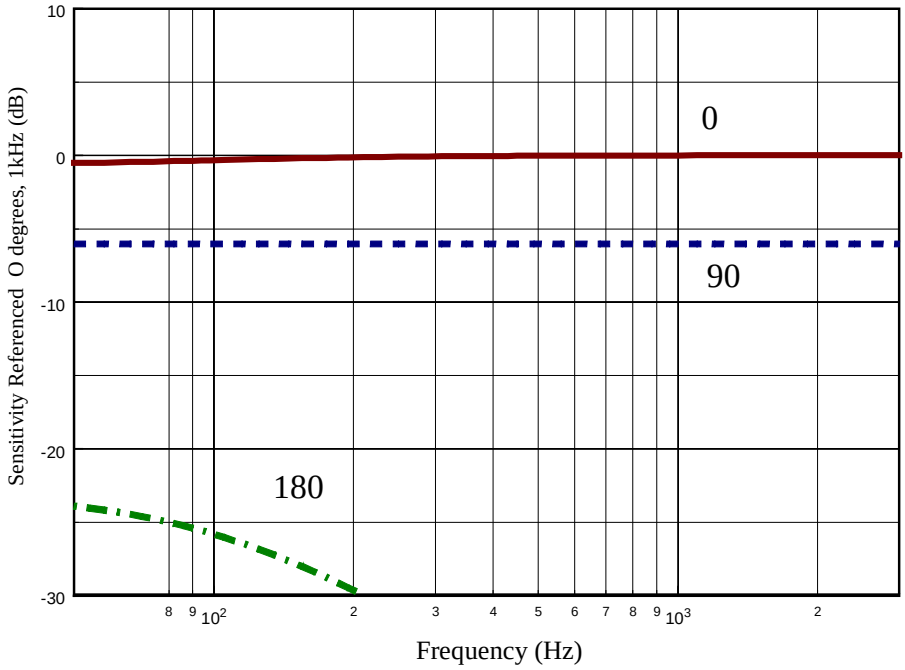

Fig. 14. Frequency Response, Dual-Diaphragm Model, 2 Feet Source Distance.

Fig. 15 shows the single-diaphragm model frequency response for a 6 inch source distance. Compared to the 2 feet source distance result, at low frequencies the 180 degree incidence response is even higher, and the 0 degree incidence response is boosted even more. This indicates a further shift in the directionality towards bidirectional. Thus, the low-pass term of the transfer function has a significant effect at this distance.

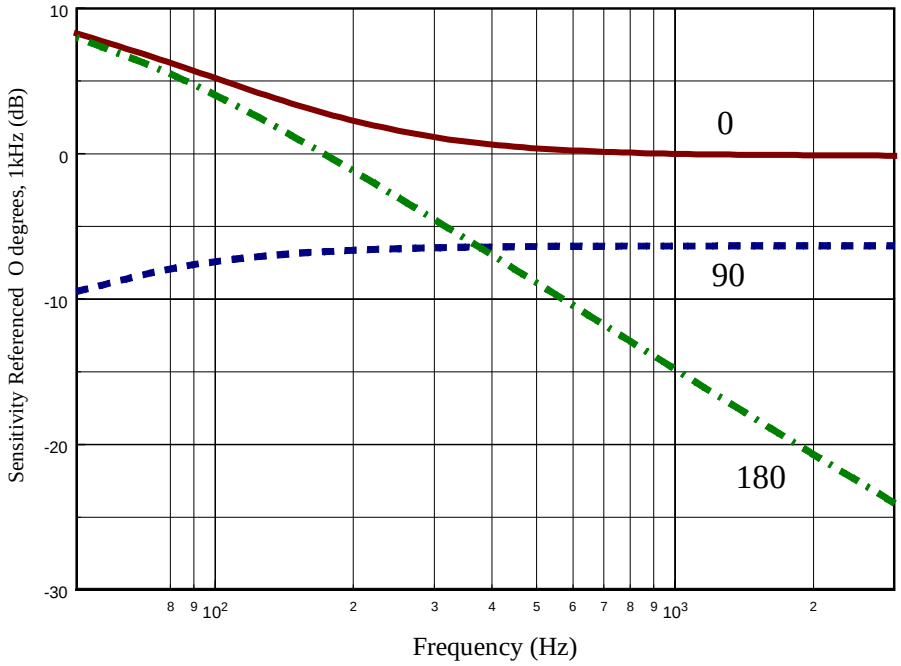

Fig. 15. Frequency Response, Single-Diaphragm Model, 6 inch Source Distance.

Fig. 16 shows the dual-diaphragm model frequency response for a 6 inch source distance. At low frequencies, the relatively high response for 180 degree incidence and the boost in the 0 degree incidence response relative to the 90 degree response indicates a shift in directionality towards bidirectional. As discussed before, this is due to the stronger influence and the change in directionality of the low-pass term of the transfer function from cardioid towards bidirectional.

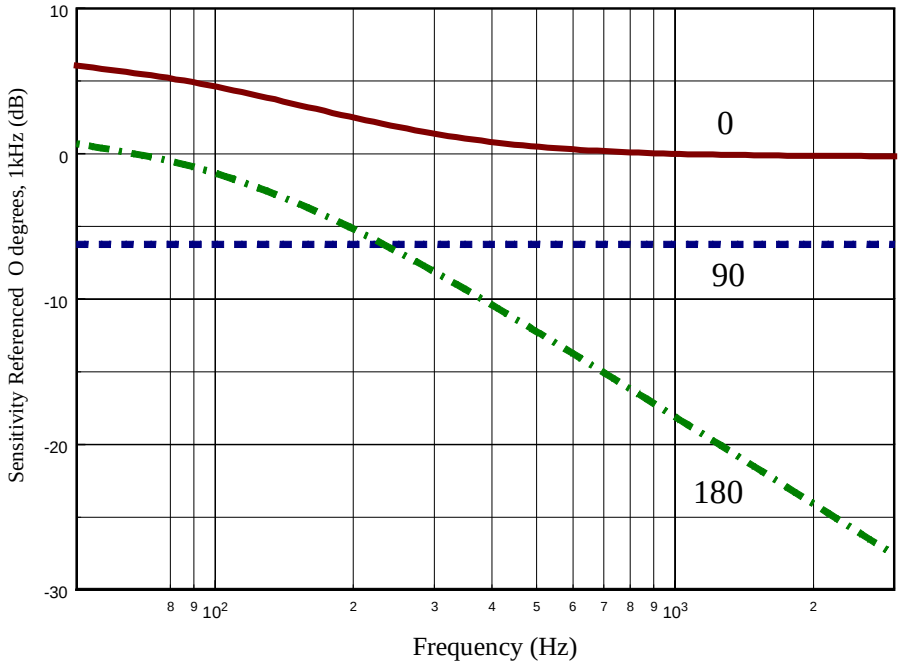

Fig. 16. Frequency Response, Dual-Diaphragm Model, 6 inch Source Distance.

5. MEASURED DATA

In order to verify the results of the models, a dual-diaphragm capsule with a geometry similar to that shown in Fig. 5 was constructed, and its frequency and polar responses were measured at same three distances used to generate the theoretical data (8 feet, 2 feet, and 6 inches). Next the rear diaphragm was cut out to create a single-diaphragm capsule having the same geometry as that shown in Fig. 1 (in the frequency range of interest, the rear back plate has no significant acoustic effect) and the same set of measurements were run. The results are shown in Figs. 17 to 23. Actual capsule parameters vary from the previous theoretical models. The trends in directionality changes as a function of distance will be demonstrated.

Figs. 24 and 25 contain the measured polar responses of single- and dual-diaphragm microphones made by two other manufacturers. The same trends in source dependent directivity are evident. In the far field the dual-diaphragm capsules display a response that is approaching omnidirectional in the low frequency range, while the single-diaphragm capsules display a more ideal polar response. Closer to the source the dual-diaphragm capsules display a near perfect cardioid in the low frequency range, while the single-diaphragm capsules start to approach a figure-of-eight pattern.

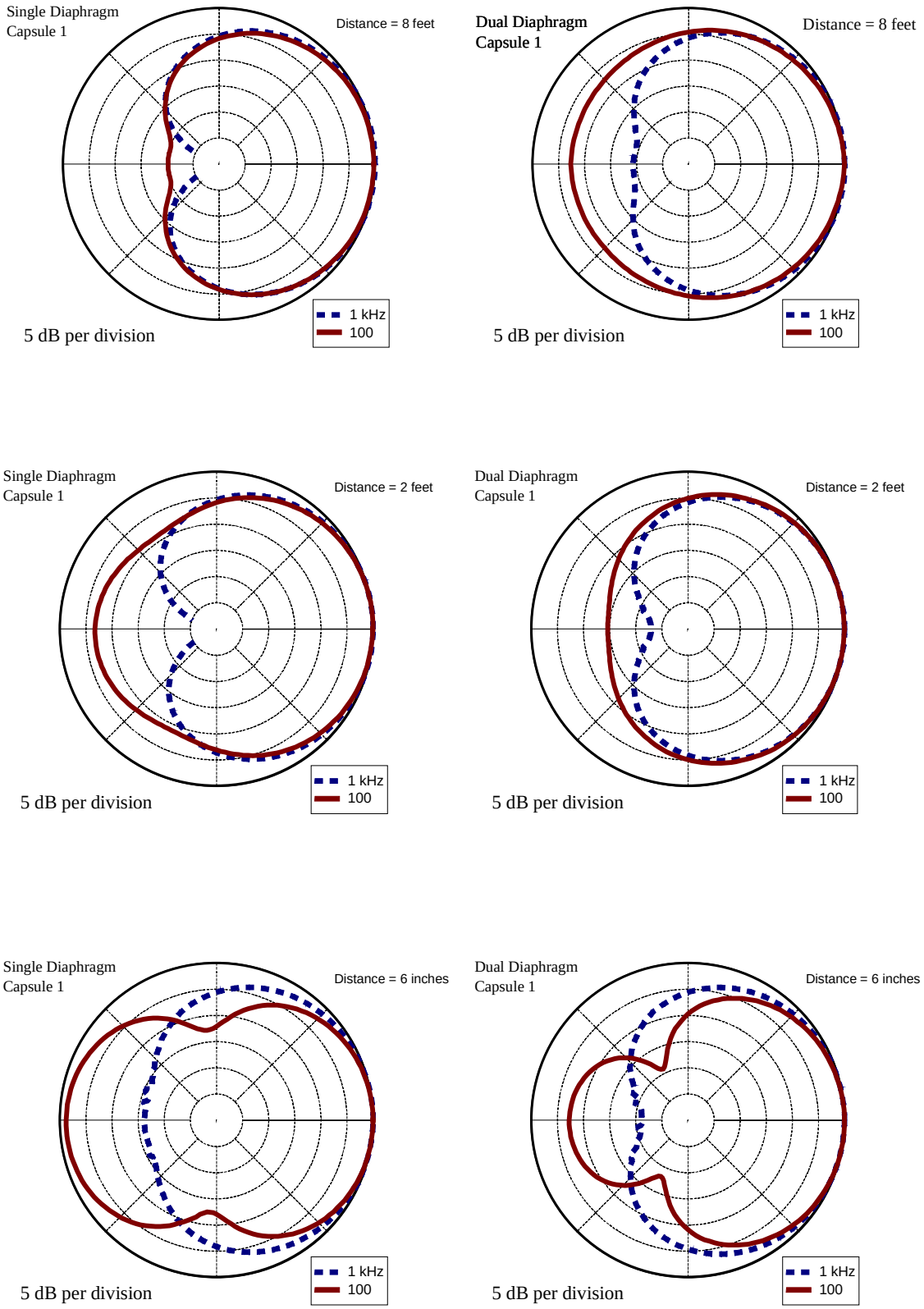

Fig. 17. Measured Polar Responses, Experimental Single- and Dual-Diaphragm Capsules.

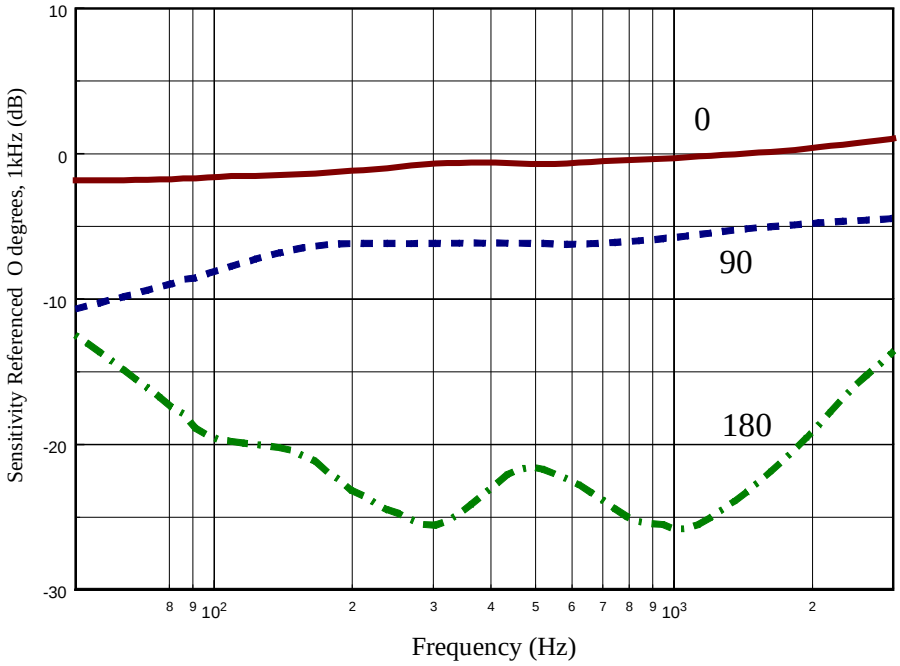

Fig. 18. Measured Frequency Response, Experimental Single-Diaphragm Capsule, 8 feet Source Distance

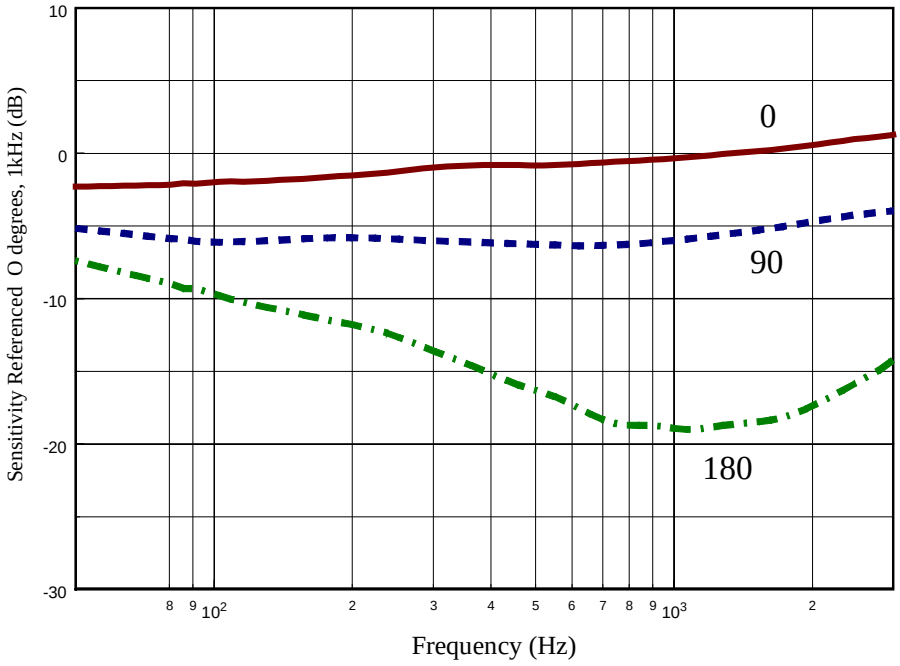

Fig. 19. Measured Frequency Response, Experimental Dual-Diaphragm Capsule, 8 feet Source Distance

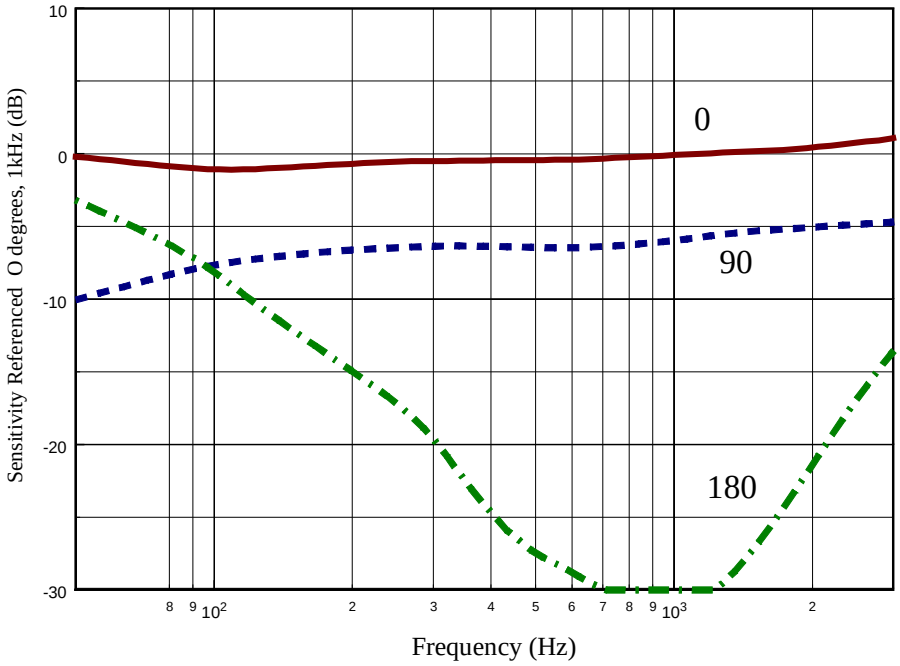

Fig. 20. Measured Frequency Response, Experimental Single-Diaphragm Capsule, 2 feet Source Distance

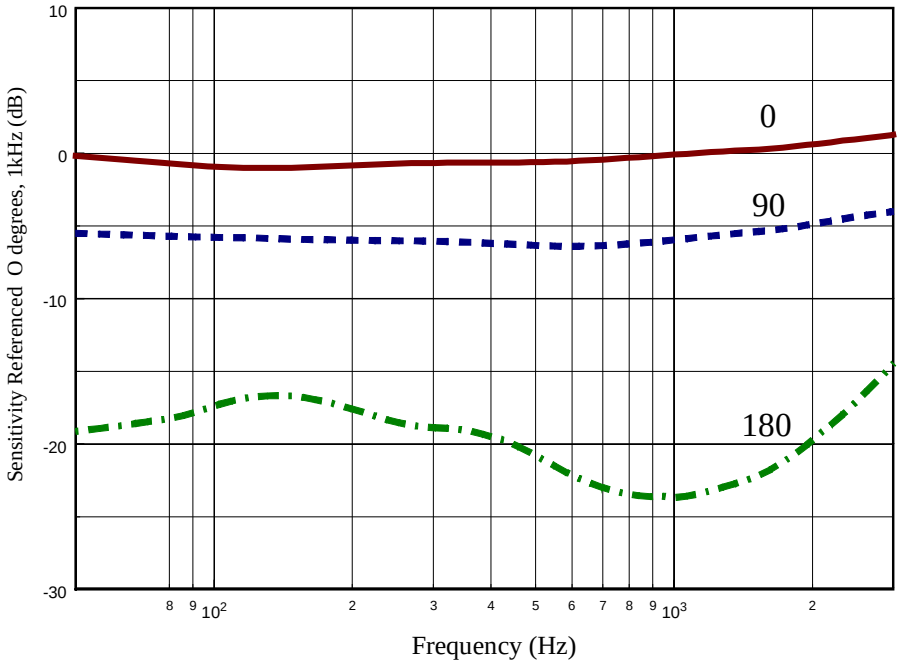

Fig. 21. Measured Frequency Response, Experimental Dual-Diaphragm Capsule, 2 feet Source Distance

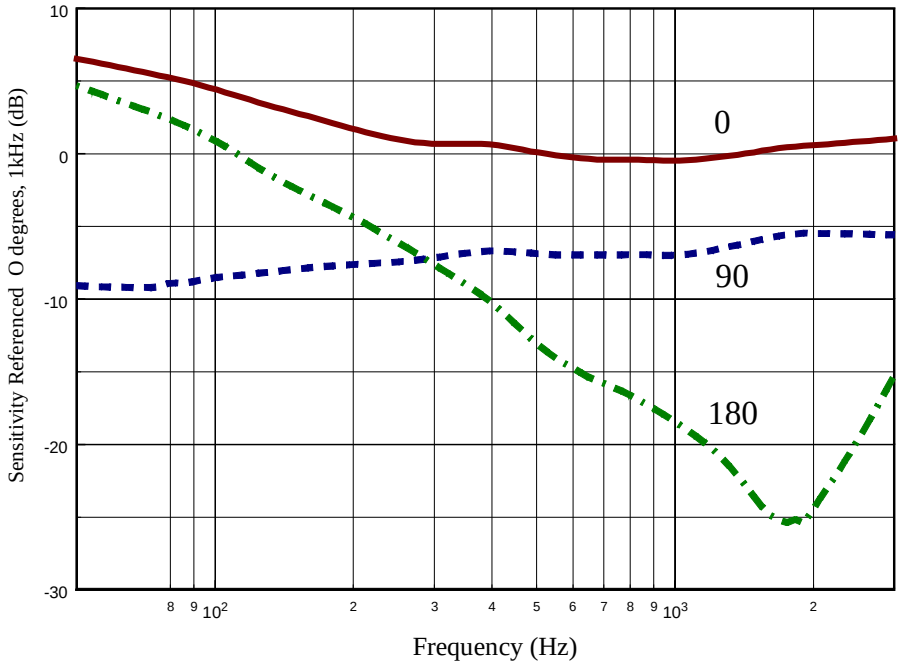

Fig. 22. Measured Frequency Response, Experimental Single-Diaphragm Capsule, 6 inch Source Distance

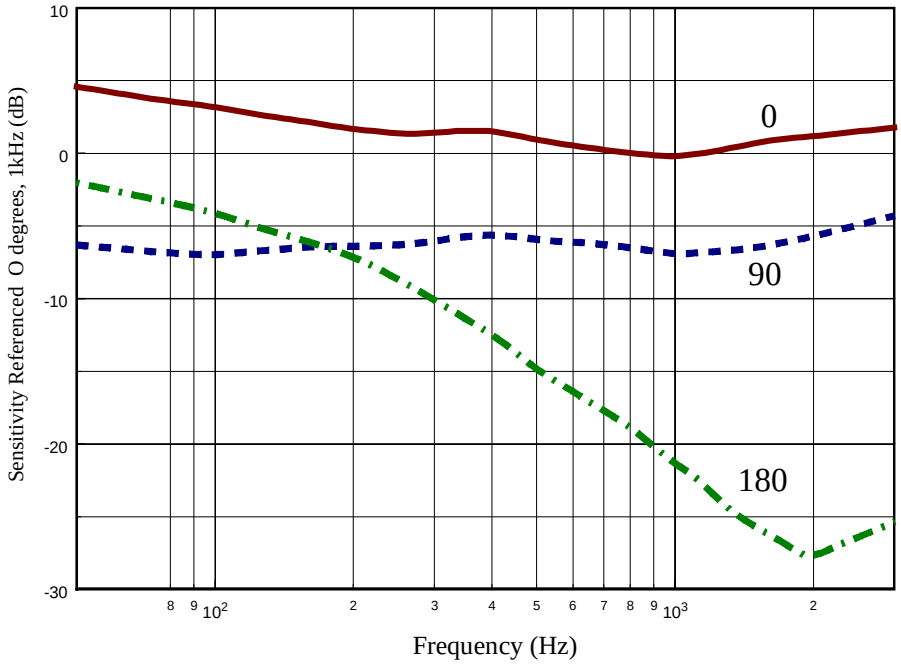

Fig. 23. Measured Frequency Response, Experimental Dual-Diaphragm Capsule, 6 inch Source Distance

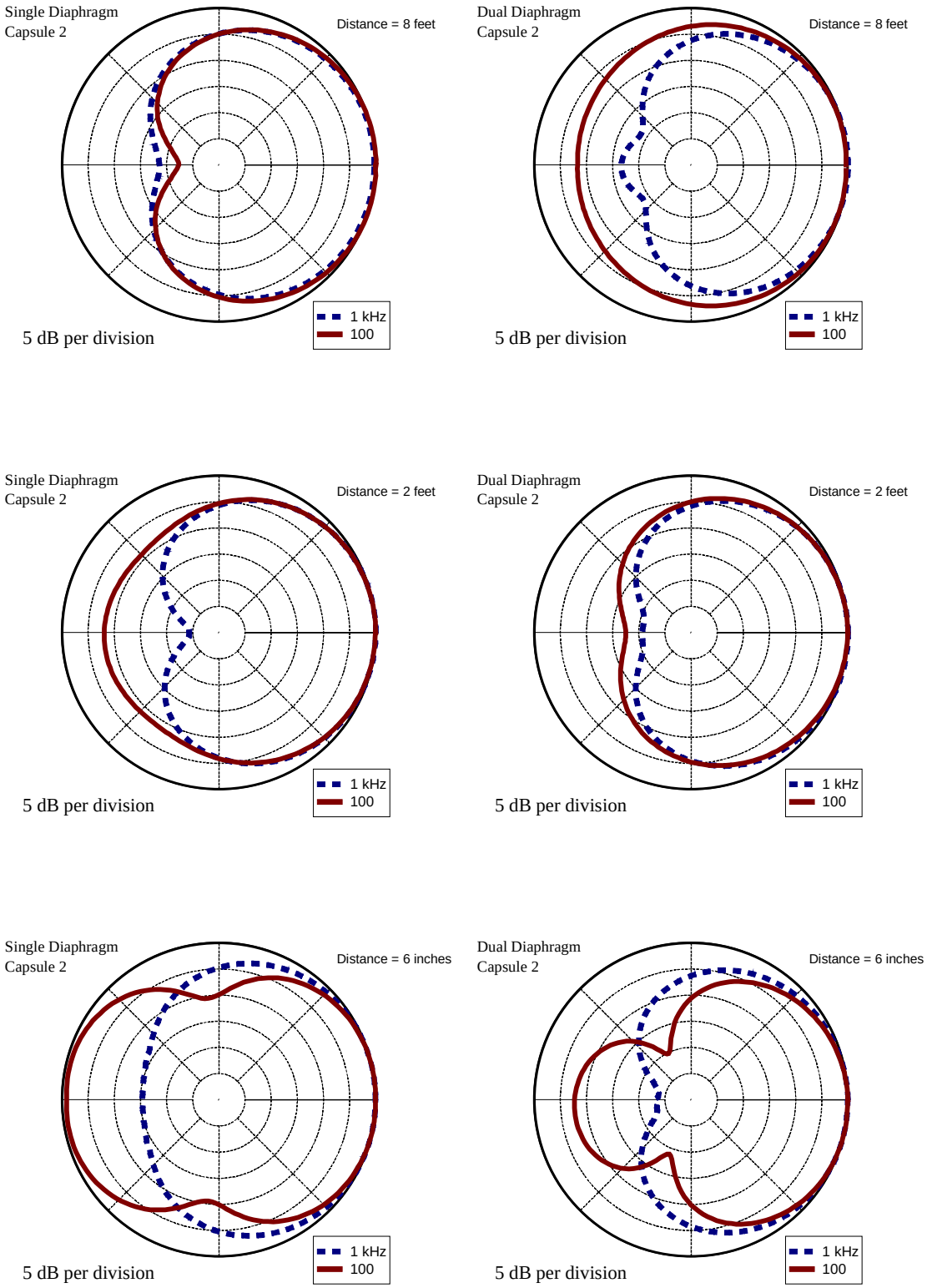

Fig. 24. Measured Polar Responses, Manufacturer #2 Single- and Dual-Diaphragm Microphones.

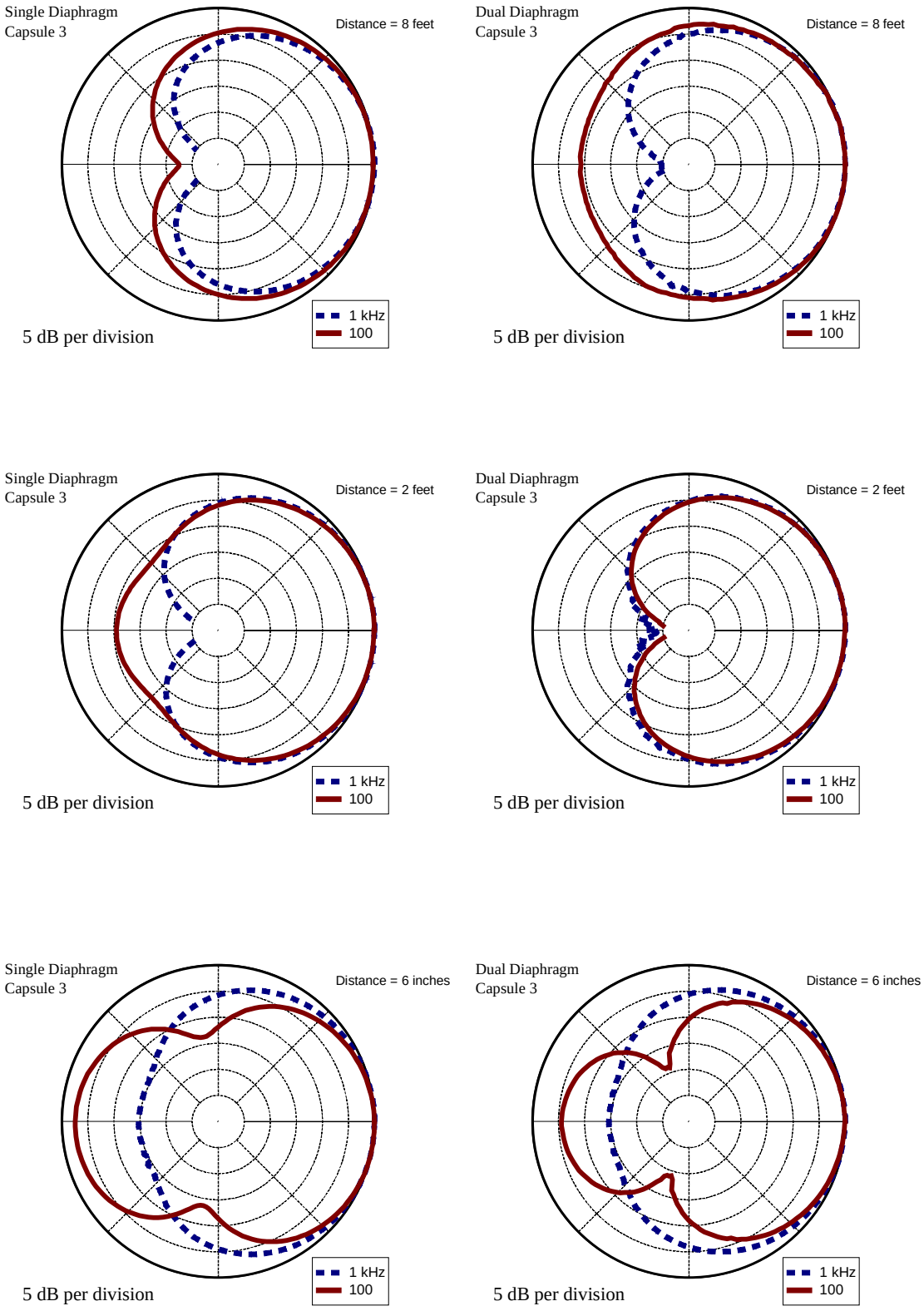

Fig. 25. Measured Polar Responses, Manufacturer #3 Single- and Dual-Diaphragm Microphones.

6. POP PERFORMANCE

Pop measurements using the current IEC technique [3] were made on the experimental capsules discussed in the previous section. Measurements were made before and after the rear diaphragm was removed. Un-weighted measurements were used in order to capture the dominance of the low frequency energy. This technique was similarly employed in [4]. Fig. 26 shows the third-octave energy in a pop measurement of both the dual- and single-diaphragm experimental capsules.

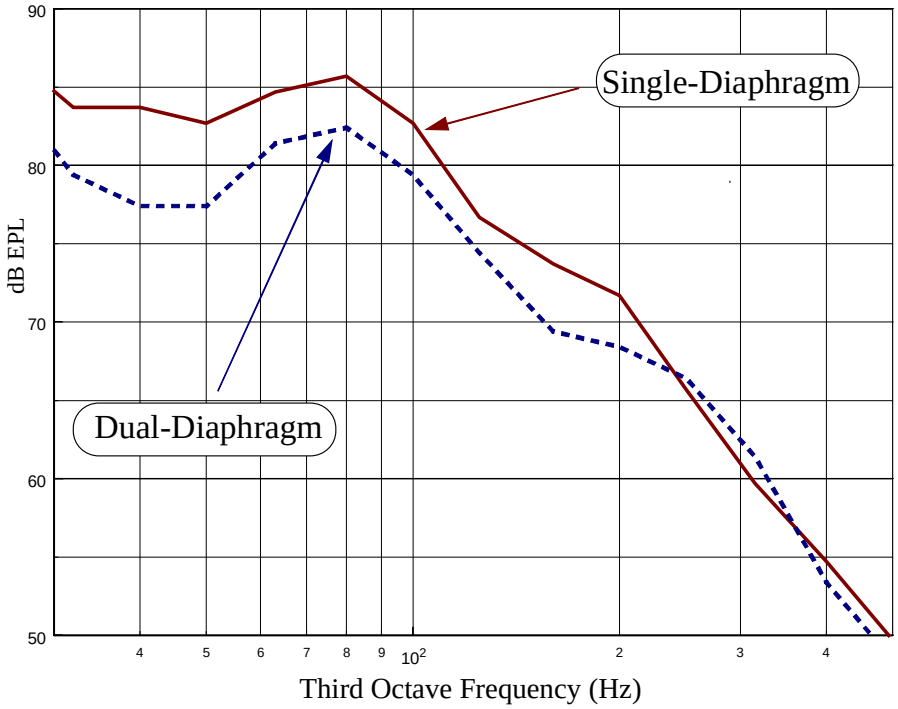

Fig. 26. Dual- and Single-Diaphragm Capsule Pop Measurements.

The resulting equivalent pop levels (EPL) are

Dual-Diaphragm Capsule, 91 dB EPL (unweighted),

Single-Diaphragm Capsule, 95 dB EPL (unweighted).

The measurements were performed with the capsules 10 cm (approximately four inches) from the pop source. As shown previously, in the frequency range below 100 Hz, for sources in close proximity the single-diaphragm capsule has a polar response closer to bidirectional than the dual-diaphragm capsule. Also, the single-diaphragm capsule exhibits a larger boost in low-frequency response for sources in close proximity. These characteristics indicate the single-diaphragm capsule is more pressure-gradient sensitive, and as such would be more sensitive to pop.

7. MULTIPATTERN OPERATION

Fig. 27 displays the front and back cardioid polar pattern orientations for multi-pattern operation. The front cardioid output is taken from the front diaphragm and back plate, while the back output is taken from the back diaphragm and back plate.

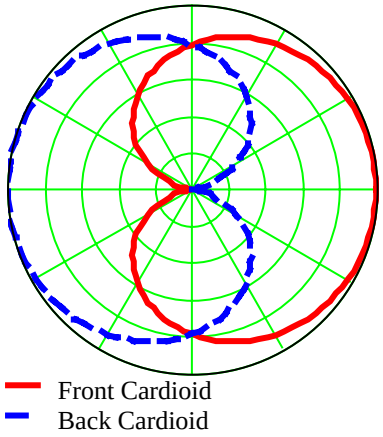

Fig. 27. Cardioid Configuration for Multi-Pattern Operation (5 dB per division).

The complete range of first order polar patterns (from omnidirectional to bidirectional) are obtained using the following summing strategy.

$$e_{out} = front\_cardioid + K(back\_cardioid), \text{ where } -1 \le K \le 1 \quad (10)$$

To obtain an omnidirectional pattern, the front and back cardioid patterns are simply added to together (K=1). To obtain a bidirectional pattern the cardioids are added together with opposite polarity (K=-1) resulting in the polar patterns illustrated in fig. 28.

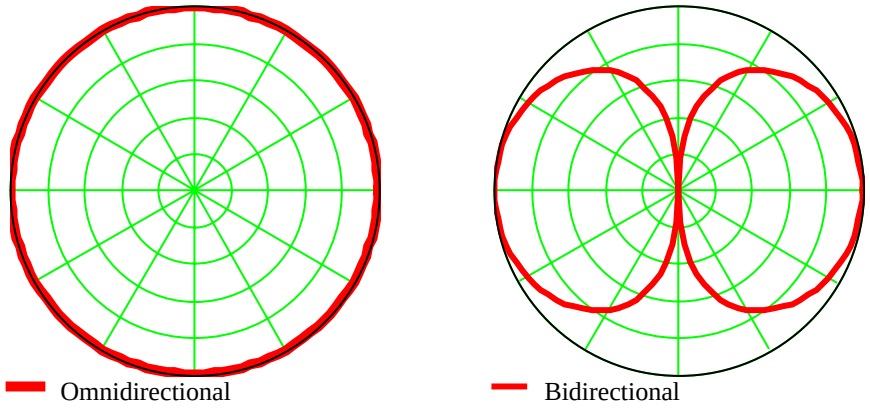

Fig. 28. Multi-pattern Omnidirectional and Bidirectional Polar Plots (5dB per division).

How does the low frequency proximity dependent behavior of dual-diaphragm cardioids effect the resulting patterns? For the omnidirectional and bidirectional cases, the polar patterns turn out to be unaffected. On the other

hand, there is an effect on the resulting on-axis frequency sensitivity for the bidirectional case, while the omnidirectional pattern maintains flat frequency sensitivity in the low frequency range regardless of source distance. The following measurements of the experimental dual-diaphragm capsule, summed appropriately for multi-pattern operation, at 8 feet display these results. At far field distances the omnidirectional maintains a flat response and is independent of source distance. On the other hand, at closer distances the low frequency response of the bidirectional increases.

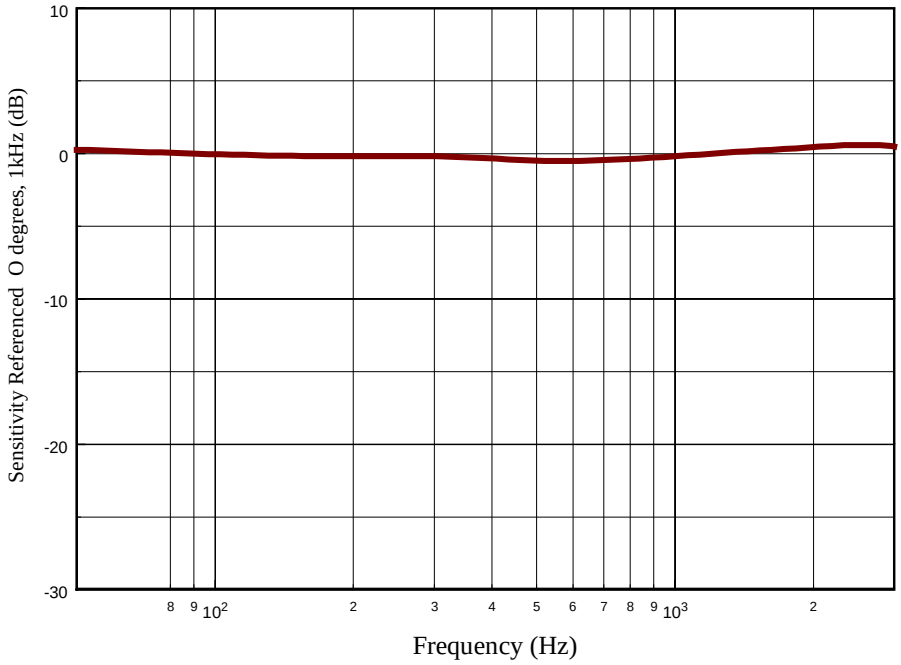

Fig. 28. Dual-Diaphragm Omnidirectional Constant at all Distances (On-Axis).

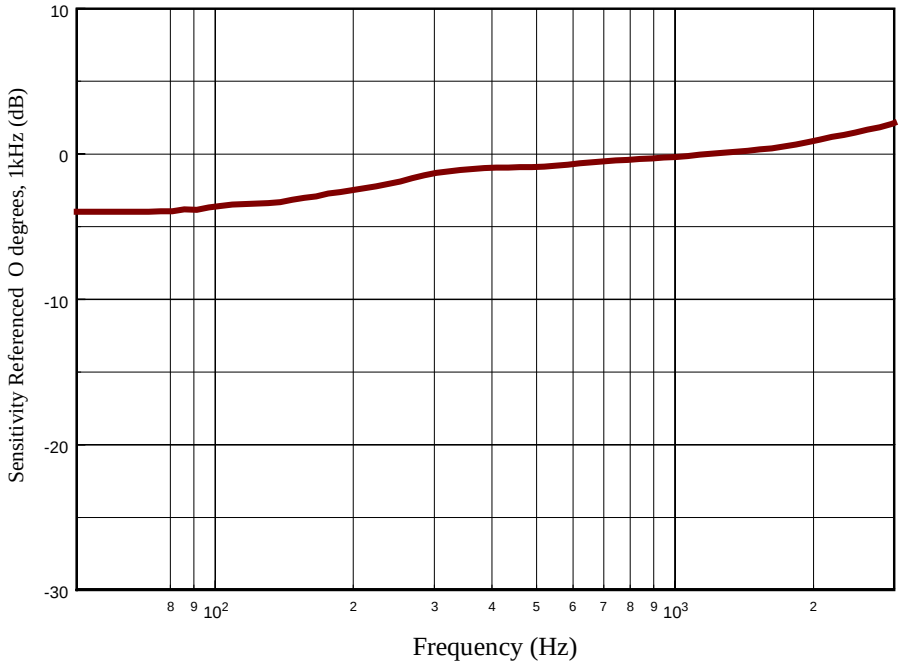

Fig. 29. Dual-Diaphragm Bidirectional at 8 feet (on-axis).

Since the bidirectional pattern is obtained by taking the difference in the front and back cardioid capsule responses, the sensitivity differences in the low frequency range of the cardioid patterns will be magnified in the bidirectional. The following plots illustrate this behavior by modeling the on-axis response of both the cardioid and the bidirectional and three different distances. This trend has also been confirmed with measured results.

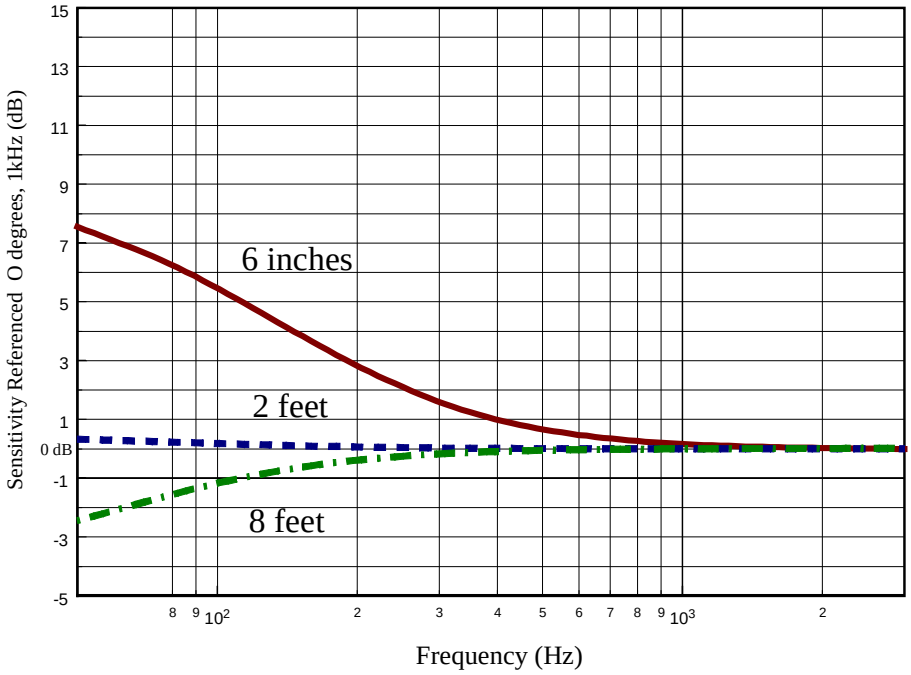

Fig. 30. Modeled Dual-Diaphragm Cardioid at different distances.

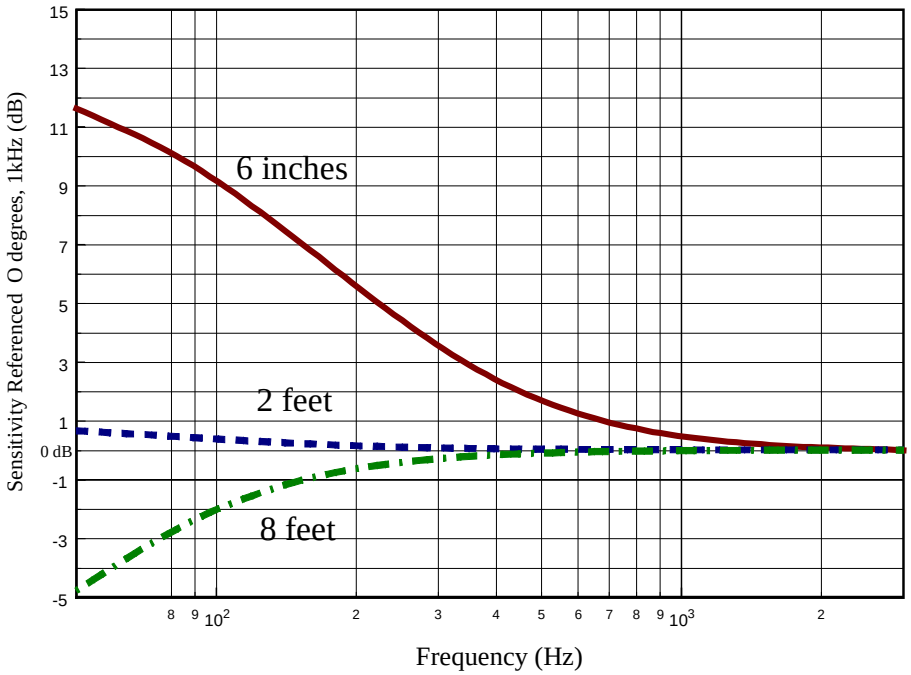

Fig. 31. Modeled Dual-Diaphragm Bidirectional at different distances.

Future work in this area would include an investigation of the other intermediate first order patterns such as super-cardioid, hyper-cardioid, and sub-cardioid.

8. DISCUSSION AND CONCLUSIONS

It has been shown, through both theoretical and experimental demonstrations, that single- and dual-diaphragm cardioid condenser capsules respond differently to low frequency sound sources. This can be attributed to the difference in the acoustic phase shift network, which for the dual-diaphragm capsule has the rear diaphragm as the first element. This diaphragm acts as a compliance at low frequencies (Fig. 6), and as such its impedance gets larger as frequency is lowered, partially blocking low frequency sound waves from reaching the back of the diaphragm. It follows that at lower and lower frequencies the dual-diaphragm capsule acts less as a pressure-gradient responding device and more like a pressure responding device. One real effect is that at a given source distance, the dual-diaphragm capsule has a polar response that is less directional than its single-diaphragm counterpart. Also, the dual-diaphragm capsule has reduced proximity effect and pop sensitivity.

This difference in low frequency directionality between dual- and single-diaphragm capsules translates into inherent advantages and disadvantages for near- and far-field applications. In the far-field, the single-diaphragm capsule has superior polar and on-axis responses, rejecting low-frequency rear-incident sound waves better and reproducing front-incident sound more accurately. The dual-diaphragm capsule has a low frequency directional behavior that is more suited for close distance applications where both the desired front-incident sound and unwanted rear-incident sound are in the near field. For intermediate distances either design might be suitable. Traditionally dual-diaphragm designed capsules have been preferred for vocal applications with references specifically made to the low frequency character. The findings of this paper offer a theoretically bases for this evident differentiation.

Every time a microphone is used, a three-dimensional sound field is integrated down to a one-dimensional signal. New knowledge on how transducer performance is effected by source distance can serve as a basis for new microphone characterization formats currently under consideration in the AES Microphone Characterization Committee SC-04-04. Ultimately, the goal is to provide the end user with application specific information.

REFERENCES

[1] Von Braunmuhl and Weber, U.S. Patent 2,179,361 (1939); filed 1936 Mar. 30.

[2] Torio, G. , “Understanding the Transfer Function of Condenser Microphones in Response to Different Sound Sources”, 105th AES Convention, San Francisco, September 26th, 1998.

[3] IEC 60268-4: Sound System Equipment – Part 4: Microphones: Appendix B.

[4] Schneider, M. “Pop Measurements, Low Frequency Response and Microphone Construction”, 104th AES Convention, Amsterdam, 1998.

APPENDIX: DUAL-DIAPHRAGM CONDENSER CAPSULE MODEL DERIVATION

Strategy:

Solve for volume velocity U as a function of P_f and P_b
Substitute in the expression for P_b as a function of P_f for a point source
Solve for the output voltage e_o as a function of the front capsule pressure, P_f

Referring to Fig. 6 and using superposition to solve for U as a function of P_f and P_b gives

$$U\left(P_f, P_b\right) = U\left(P_f\right)\Big|_{P_b=0} + U\left(P_b\right)\Big|_{P_f=0} \quad . \tag{A1}$$

Solving for of U as a function of P_f results in the expression

$$U\left(P_f\right)\Big|_{P_b=0} = \frac{P_f}{\dfrac{1}{sC_d} + \dfrac{1}{sC_a + \dfrac{1}{R_a + \dfrac{1}{s\left(C_a + C_d\right)}}}} \quad . \tag{A2}$$

As a means of solving for U as a function of P_b, the circuit in Fig. 6 is simplified to obtain the modified equivalent circuit shown in Fig. A1.

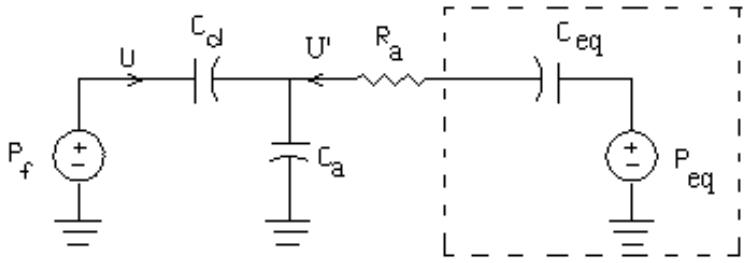

Fig A1. Modified Dual-Diaphragm Capsule Equivalent Circuit.

In the circuit,

$$C_{eq} = C_d + C_a \tag{A3}$$

and

$$P_{eq} = P_b\left(\frac{C_d}{C_d + C_a}\right). \tag{A4}$$

The expression

$$U(P_b)\big|_{P_f=0} = U'(P_b)\big|_{P_f=0} \cdot \frac{U(P_b)}{U'(P_b)}\bigg|_{P_f=0} \tag{A5}$$

is used as an intermediate step. Solving the circuit and substituting in (A3) and (A4) gives

$$U'(P_b)\big|_{P_f=0} = P_b \frac{\dfrac{C_d}{C_d + C_a}}{\dfrac{1}{s(C_d + C_a)} + R_t + \dfrac{1}{s(C_d + C_a)}} \tag{A6}$$

and

$$\frac{U'(P_b)}{U(P_b)}\bigg|_{P_f=0} = \frac{-\dfrac{1}{sC_t}}{\dfrac{1}{sC_t} + \dfrac{1}{sC_d}} \quad . \tag{A7}$$

Substituting (A6) and (A7) into (A5), and then substituting the result and (A2) into (A1) gives

$$U = P_f \frac{1}{\dfrac{1}{sC_d} + \dfrac{1}{sC_a + \dfrac{1}{R_a + \dfrac{1}{s(C_a + C_d)}}}} - P_b \frac{\dfrac{C_d}{(C_a + C_d)}}{R_a + \dfrac{2}{s(C_a + C_d)}} \cdot \frac{\dfrac{1}{sC_a}}{\dfrac{1}{sC_a} + \dfrac{1}{sC_d}} \quad . \tag{A8}$$

Simplifying results in the expression

$$U = \frac{P_f\left[s^2 R_a C_a C_d + s\left(C_d + \dfrac{C_t}{C_a + C_d}\right)\right] - P_b\left[s\left(\dfrac{C_d^2}{C_a + C_d}\right)\right]}{sR_a(C_a + C_d) + 2} \quad . \tag{A9}$$

For a point source, the expression relating the sound pressure at the back of the capsule to the sound pressure at the front of the capsule is [1]

$$P_b = P_f\left[1 - \frac{sd}{c}\cos(\theta) - \frac{d}{r}\cos(\theta)\right] . \tag{A10}$$

In this expression ***c*** is the speed of sound and ***r*** is the distance from the source.

Substituting (A10) into (A9) and simplifying gives

$$\frac{U}{P_f} = \frac{s^2 \frac{R_a C_a C_d}{2}\left(1 + \frac{d}{cR_a\left(C_a + \frac{C_a^2}{C_d}\right)}\cos(\theta)\right) + s\frac{C_d C_a}{C_d + C_a}\left(1 + \frac{d}{r}\frac{C_d}{2C_a}\cos(\theta)\right)}{sR_a\frac{C_d + C_a}{2} + 1}. \quad \text{(A11)}$$

The output voltage signal is related to the volume velocity by the expression

$$e_o = K_{AE}\frac{U}{s}, \quad \text{(A12)}$$

where K_{AE} is an electrical to acoustical coupling factor. Substituting (A12) into (A11) and rearranging results in the transfer function

$$\frac{e_o}{P_f} = K_{AE}\frac{C_d C_a}{C_d + C_a}\frac{s\frac{R_a(C_a + C_d)}{2}\left(1 + \frac{d}{cR_a\left(C_a + \frac{C_a^2}{C_d}\right)}\cos(\theta)\right) + \left(1 + \frac{d}{r}\frac{C_d}{2C_a}\cos(\theta)\right)}{sR_a\frac{C_d + C_a}{2} + 1}. \quad \text{(A13)}$$

This equation is in the form of the general expression for summed first order low-pass and high-pass filters. As such, it can be rewritten symbolically as

$$\frac{e_o}{P_f} = K_{AE}K_C\frac{K_{HP\_DD}\left(\frac{s}{2\pi f_{o\_DD}}\right) + K_{LP\_DD}}{\left(\frac{s}{2\pi f_{o\_DD}}\right) + 1}. \quad \text{(A14)}$$

K_C is the common gain term (series connection of C_d and C_a) given by the expression

$$K_C = \frac{C_d C_a}{C_d + C_a}. \quad \text{(A15)}$$

f_{o_DD} is the cutoff frequency for both the high-pass and low-pass filters, and is given by the expression

$$f_{o\_DD} = \frac{1}{\pi\left[R_a\left(C_a + C_d\right)\right]} \ . \tag{A16}$$

K_{HP_DD} is the high-pass filter gain, and is given by the expression

$$K_{HP\_DD} = \left(1 + \frac{d}{cR_a\left(C_a + \frac{C_a^2}{C_d} \right)} \cos(\theta) \right) . \tag{A17}$$

K_{LP_DD} is the low-pass filter gain, and is given by the expression

$$K_{LP\_DD} = \left(1 + \frac{d}{r} \frac{C_d}{2C_a} \cos(\theta) \right) \ . \tag{A18}$$